Journal of Applied Sciences Research, 9(8): 4709-4808, 2013
ISSN 1819-544X
This is a refereed journal and all articles are professionally screened and reviewed

ORIGINAL ARTICLES

The Effect of Nano- Materials on The Characteristics and Performance of Aromatic Polyamide Membranes and Its Use in Groundwater Desalination in the Area Between Safaga and El-Quseir – Egypt.

[1]M.A. Gomaa, [1]A.A. Hamouda, [1]M.E. Abdelfattah, [2]M.M. Emara and [2]M.M.B. El-Sabbah

[1]Desert Research Center, Hydrogeochemistry Dept., Egypt
[2]Al-Azhar University, Faculty of science, Chemistry Dept., Egypt

ABSTRACT

The thin film zeolite nanocomposite (TFNC) membranes were coated via interfacial polymerization of trimesoyl chloride (TMC) and m-phenylenediamine (MPD) monomers over porous polysulfone support. Different types of nanocomposite membranes were synthesized depending zeolite loading into the polyamide film. X-ray diffraction (XRD), FT-IR, transmission electron microscopy (TEM) and scanning electron microscopy techniques were employed to study the morphology of the pure zeolite and nanocomposite membranes. The calculated grain size of zeolite nanoparticles was 5.32 to 11.57 nm. The nanocomposite membranes had higher water permeability than the pure polyamide membranes. The results showed that addition of zeolite to the polyamide membrane led to improvement of surface properties such as an increase in pore size and water flux. The nanocomposite membranes with high concentration of monomers in interfacial polymerization exhibited a high water flux and low salt rejection. Excellent membrane performance was observed for the nanocomposite membrane containing about 0.05 % (w/v) zeolite, 0.15 % (w/v) TMC and 2 % (w/v) MPD which its flux was higher by 1.45 times than the flux value of the polyamide membrane with slightly decreasing in salt rejection. The obtained results show that TFZNC membranes are suitable for groundwater desalination.

Key words: Thin film composite; zeolite nanoparticles; pure water permeability; water flux; salt rejection.

Introduction

Water is the source of life, and is essential for social and economic development. Water shortage has recently become a serious problem worldwide. Although 75% of the earth's surface is water, 97.5% of it is in oceans and is considered undrinkable without proper processing due to its high salinity. Only the remaining small 2.5% of the earth's water is considered freshwater. However, only 0.3% of the freshwater in lakes and rivers is accessible, while the remaining freshwater is deep underground or in the form of snow and ice **(**United Nation, 2009). Reverse osmosis (RO) membranes have become a water desalination technology, which promises to greatly increase the supply of clean water through purification of nontraditional water sources. Thin film composite (TFC) membranes are widely uses in most desalination plants due to its high water flux and salt rejection. One of the most frequently used TFC membranes is the polyamide composite membrane with skin barrier layer which is created by the interfacial polymerization technique between two reactive monomers on the top of polysulfone porous support membrane **(**Singh *et al.*, 2006 & Ghosh and Hoek 2009 & Pendergast *et al.*, 2010). The trimesoyl chloride (TMC), m-phenylenediamine (MPD) monomers have been used in polyamide layers in a number of research studies and an attempt has been made to improve this membrane performance. For example, investigating the effective parameters of polymerization such as solvent, reaction time, temperature on membrane performance (Ghosh *et al.*, 2008 & Kim *et al.*, 2002 & Liu *et al.*, 2007 and Gilron *et al.*, 2001), sub layer effect on water permeability and salt rejection, surface modification by grafting hydrophilic materials for decreasing membrane fouling (Roh *et al.*, 1998 and Yu *et al.*, 2009), changing one of the monomers, increasing water permeability, salt rejection and chlorine resistance (Liu *et al.*, 2006 & Rawajfeh, 2005 & Zhou *et al.*, 2005 & Jeong *et al.*, 2007 and Kim *et al.*, 2003) and using nano material into polyamide thin film nanocomposites (Soroko and Livingston, 2009 & Jadav *et al.*, 2010 & Jadav and Singh, 2009 & Wu *et al.*, 2009 & Lind *et al.*, 2009).

The innovations in RO membrane materials include; increasing water permeability for energy savings, improving control of selectivity in membrane design and more fouling resistant surfaces (Clark *et al.*, 1998). The incorporation of zeolite in a polymeric membrane is able to improve the separation performance of the membrane due to the combined effect of molecular sieving action, selective adsorption and difference in

Corresponding Author: M.E. Abdelfattah, Desert Research Center, Water desalination unit, Hydrogeochemistry Dept., Egypt
E-mail: mohameddrc1983@yahoo.com

diffusion rates. Moreover, zeolites possess high mechanical strength, good thermal and chemical stability, and thus, the resulting filled membranes can be used over a wide range of operating conditions.

The hydrophilic nano-zeolite was incorporated in the polyamide layer to modify membrane transport properties which resulted in membranes with dramatically improved permeability when compared to pure polyamide membranes (Jeong *et al.*, 2007). Lind *et al.*, 2009 observed that nanoparticle size may be considered an additional "degree of freedom" in designing thin film nanocomposite of reverse osmosis membranes and mobile cation plays an important role in water permeability in similar salt rejection. The incorporation of nano-zeolite-A in polyamide (PA) is used to increase water permeability through the enhanced hydrophilicity in the membranes.

This paper aims to prepare TFC and TFZNC membranes using modified interfacial polymerization technique. The effects of the zeolite nano-particle addition on the properties of TFC membrane such as pure water permeability (L_P), water flux (J_w) and salt rejection (Rs %) were examined.

2. Experimental:

2.1. Materials:

Polysulfone beds (Udel P 3500 LCD MP7, MW= 77000, Mn=22000); N, N`-Dimethylacetamide (DMAc); 1, 3, 5-Benzenetricarbonyl trichloride (TMC) (>98%); m-phenylenediamine (MPD) (> 99%); triethylamine (TEA); camphor sulphonic acid (CSA) and sodium lauryl sulphate (SLS) were purchased from Sigma–Aldrich and used as received, natural zeolite were obtained from England.

2.2. Methods:

2.2.1. Preparation of zeolite nanoparticles:

The zeolite nanoparticles were prepared from zeolite microcrystals by grinding method. A specific amount of microcrystal zeolite powder was loaded in the grinding machine for a milling time of 3 hr. Then milled powder was dispersed in an aqueous solution under ultrasonication for 30 min, and then the large zeolite particles were removed by centrifugation at 2000 rpm for 20 min. The small zeolite crystals were recovered by centrifugation at 5000 rpm for 30 min, and then the recovered products were dried at 120°C for 1 day. Finally, the products were stored in a dry box for use in polymer membrane preparation

2.2.2. Preparation of TFC membranes:

TFC and TFZNC membranes were prepared on the surface of Ps support using modified interfacial polymerization technique. PS casting solution was prepared by phase inversion method according to (Huan *et al.*, 2009) , dissolve 15 wt. % PS bead, in N,N-Dimethylacetamide as a suitable solvent at 70-80°C with constant stirring until homogenous solution was obtained. After that, the solution was casted on a flat and horizontal glass plate. The membrane was allowed to dry and the solvent was slowly evaporated in an air for 30 sec. The casting and evaporation processes followed by precipitation in a coagulation (water) bath during the PS casting the conditions were kept at room temperature. The membranes were removed from the coagulation bath and washed thoroughly with distilled water to remove residual solvents and kept wet until use.

TFC membranes were synthesized via interfacial polymerization technique (Cadotte *et al.*, 1980 & Cadotte, 1981 and Sanchuan *et al.*, 2009**)** with some modification using MPD aqueous solution and TMC in hexane solution. The aqueous MPD solution (2 %) containing additives (TEA: CSA: SLS in ratio of 2:4:0.1 w/v %) was poured onto the top surface of the supporting PS layer and allowed to soak for 2 minutes. Excess solution was drained off the surface using soft rubber until no excess MPD droplets exist. Organic solution of TMC (0.15 %) was poured onto PS membrane which saturated with MPD. After 60 second, the excess organic solution was removed off the surface, the reaction between MPD and TMC resulted in the formation of an ultra- thin layer of PA over the surface of PS support layer. The resulting TFC membrane was cured in an oven at 85 ^{o}C for 10 minutes to attain the desired stability of the formed structure. Finally, MPD solution was poured again onto the top surface of the TFC and allowed to soak for 2 minutes. The membranes were thoroughly washed and kept in distilled water until carrying out application studies. In preparation of TFZNC membranes, different concentrations of zeolite (0 – 0.5 w/v %) were dispersed in hexane solution of trimesoyl chloride before the interfacial poly condensation reaction takes place. Nanoparticles dispersion was obtained by ultra-sonication for 1 h at room temperature prior to interfacial polymerization.

2.2.2. Membrane characterization:

The membranes were characterized by FT-IR, X- ray diffraction, TGA and SEM. Analysis by Infrared spectroscopy was carried out using Gensis Unicam FT-IR spectrophotometer, the dimensions of the window, to which the film was fixed, were 1.5 × 3 cm. The X- ray diffraction patterns of films were measured with Philips Model PW 3710 X-ray diffraction instrument. The thermal gravimetric analysis was carried out by using Shimadzu TGA system of type TGA-30. Morphology of the composite membrane was performed with Scanning Electron Microscopy (SEM), SEM Model Quanta FEG attached with EDX Unit, with accelerating voltage 30 K.V., magnification 250 x up to 20000 and resolution for Gun.1m. Samples were coated with gold.

Reverse osmosis properties, salt rejection (R_s %) and water flux (J_w) of the prepared membranes were measured by laboratory DDS reverse osmosis system, model LAB-M20, manufactured by Alfa Laval Comp., Denmark which consists of stainless steel cylindrical vessel, 20 cm diameter and 70 cm height, with control panel. The effective membrane area is 0.018 m^2. All membranes were evaluated for water flux and salt rejection using 2000 ppm NaCl at different applied pressure. The salt rejection percent (R_s %) was calculated as the following equation:

R_s (%) = (C_f - C_p/C_f) x 100

Where C_f and C_p are the concentrations of feed and permeate water (product), respectively. The water flux (J_w) through a semi-permeable membrane was expressed in weight of the product per unit membrane area during operation time in liter ($L/m^2.h$) was calculated as the following equation;

J_w = Q/A x t

Where, Q is water permeates in liter, A is the membrane area in meter square and t is the time in hour.

Results And Discussions

3.1. Estimation the particle size of zeolite nanoparticles:

The zeolite nanoparticles were prepared from zeolite microcrystals by grinding method. X-ray diffraction tool was used to determine the average crystal dimension of zeolite powder which calculated by Scherer's eq.1 from the diffraction peaks at 2θ values of 12°, 25° and 39°, [see Fig. 4]. These most intense XRD peak was chosen to calculate the size of the particles (d) as follows;

$$d = \frac{0.9\lambda}{\beta \cos\theta}$$

Where λ is the wavelength of the X-ray (1.54 A°), β is the full width at half maximum width of the diffraction peak in radiance, θ is the diffraction angle at the maximum intensity. The calculated particle size was 9.95 nm. The TEM image recorded for the nano zeolite sample is shown in Fig. [1], which clearly indicates that the particle size within a range of 5.32 to 11.57 nm which is consistent with the results calculated from the XRD pattern. The particles size of zeolite in membrane matrix was calculated as 17.33 nm for TFZNC (0.05 w/w %) membrane, this increase may be due to some aggregation of nanoparticles on the membrane surface.

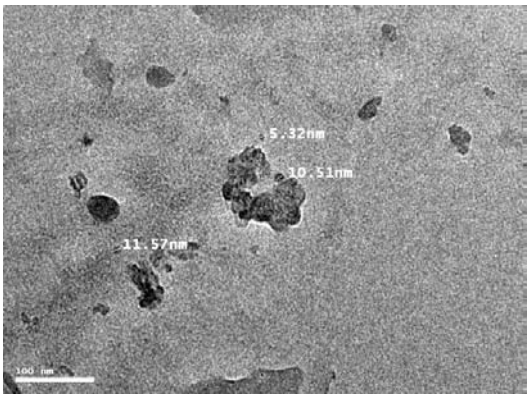

Fig. 1: TEM image of zeolite nanoparticles.

3.2. Membrane characterization:

Zeolites are a well defined class of naturally occurring crystalline aluminosilicate minerals **(**Dyer, 1988**)**, consists of an assemblage of $[SiO_4]^{-4}$ and $[AlO_4]^{-5}$ tetrahedral joined together in various regular arrangements through shared oxygen atoms, to form an open crystal lattice containing pores of molecular dimensions into

which guest molecules such as water can penetrate **(**Mortier, 1982**)**. Zeolite nanoparticles attached to PA by self-assembly between $[AlO_4]^{-5}$& $[SiO_4]^{-4}$ and carbonyl group of the polyamide, Fig [2]. This interaction can be occur through a mono dentate coordination of carbonyl group and free -COOH groups of PA to $[AlO_4]^{-5}$ & $[SiO_4]^{-4}$, binding between oxygen atoms from AlO_4 & SiO_4 with nitrogen atom of the polymer, and hydrogen bond between -NH group of PA and surface hydroxyl group of $[AlO_4]^{-5}$ & $[SiO_4]^{-4}$ **(**Lee *et al.*, 2008**)**.

The ATR-FTIR spectra of pure zeolite, TFC and TFZNC membranes are presented, Fig [3]. In spectrum of the zeolite, characteristic absorption peaks which indicate -OH stretching of water molecules in the zeolite structure, -OH groups between octahedral and tetrahedral sheets, and -OH groups on the octahedral sheet were observed at 3438 cm^{-1}, 3620 cm^{-1}, and 3695 cm^{-1}, respectively. Other characteristic peaks originating from the Si–O stretching at 1032 cm^{-1}, Al-OH bending at 913 cm^{-1}, Si–O–Al bending at 538cm^{-1}, and Si–O–Si bending at 468 cm^{-1} were also observed **(**Hasine *et al.*, 2008**)**. In the spectrum of the TFZNC, all the characteristic peaks of zeolite were observed, the absorption peaks at 3620 and 3695 cm^{-1} which correspond to the OH groups in zeolite structure disappeared. These results clearly show that high interfacial interactions existed between the zeolite layers and polymer matrix was obtained by in situ copolymerization.

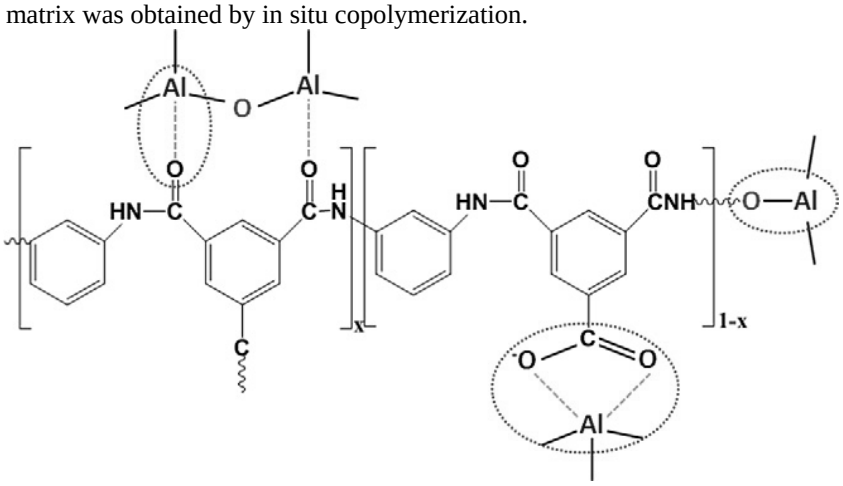

Fig. 2: Schematic representation of the interaction between PA and Zeolite nanoparticles.

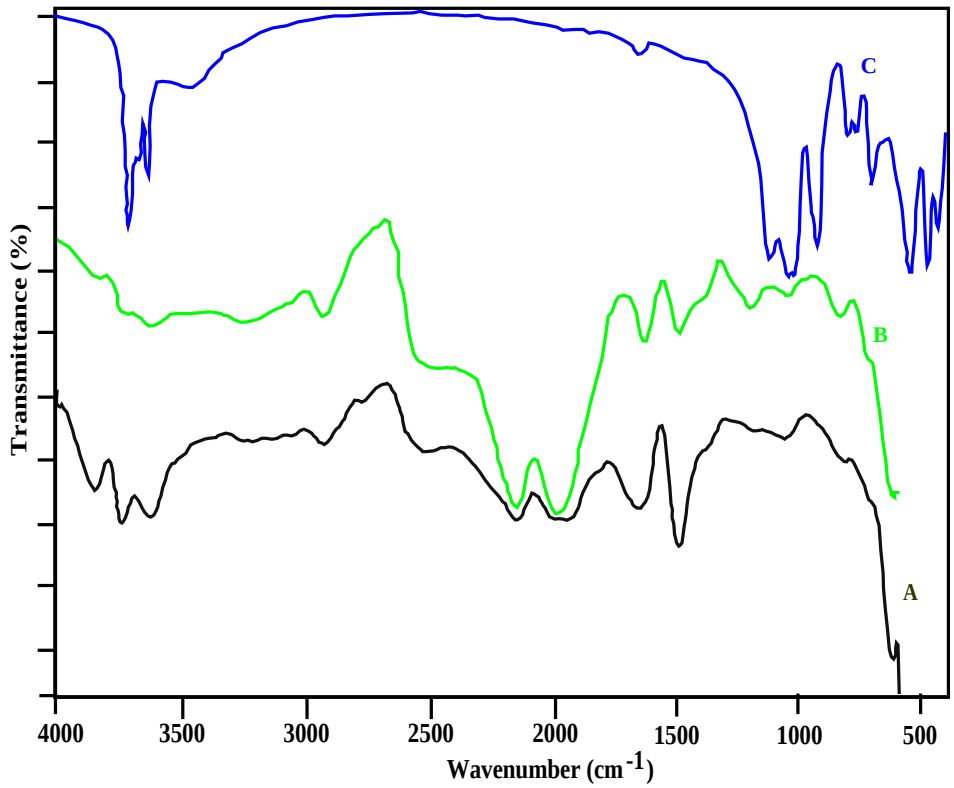

Fig. 3: AT-FTIR spectra of A) TFC, B) TFZNC (0.05 %) nanocomposite membranes and C) pure zeolite nanoparticles.

The X-ray diffraction (XRD) technique can be used to elucidate the structure of TFC and TFZNC membranes. Fig [4] shows the XRD patterns of the TFC, TFZNC and pure zeolite nanoparticles. XRD pattern of zeolite powder exhibits three well-defined characteristic peaks at 2θ =of 12.41^o, 24.91^o and 37.73^o corresponding to a d-spacing of 0.714, 0.357 and 0.238 nm, respectively. The distances between repeating layers of tetrahedral and octahedral sheets occurring in zeolite which linked by sharing oxygen atoms were calculated by the Bragg as in eq.2;

$$\lambda = 2d\sin\theta \quad (2)$$

Where λ is the wave length (0.154 nm), θ is the diffraction angle, and d is the basal space between zeolite layers, which calculated as 7.12A°. For TFZNC nanocomposite, the reflection peaks of zeolite observed with slightly shifting in addition to the dispersion peak of amorphous PA, increasing of the peak intensity and increasing of d values could be assigned to expand the zeolite layers and the intercalation of polymer chains into zeolite layers.

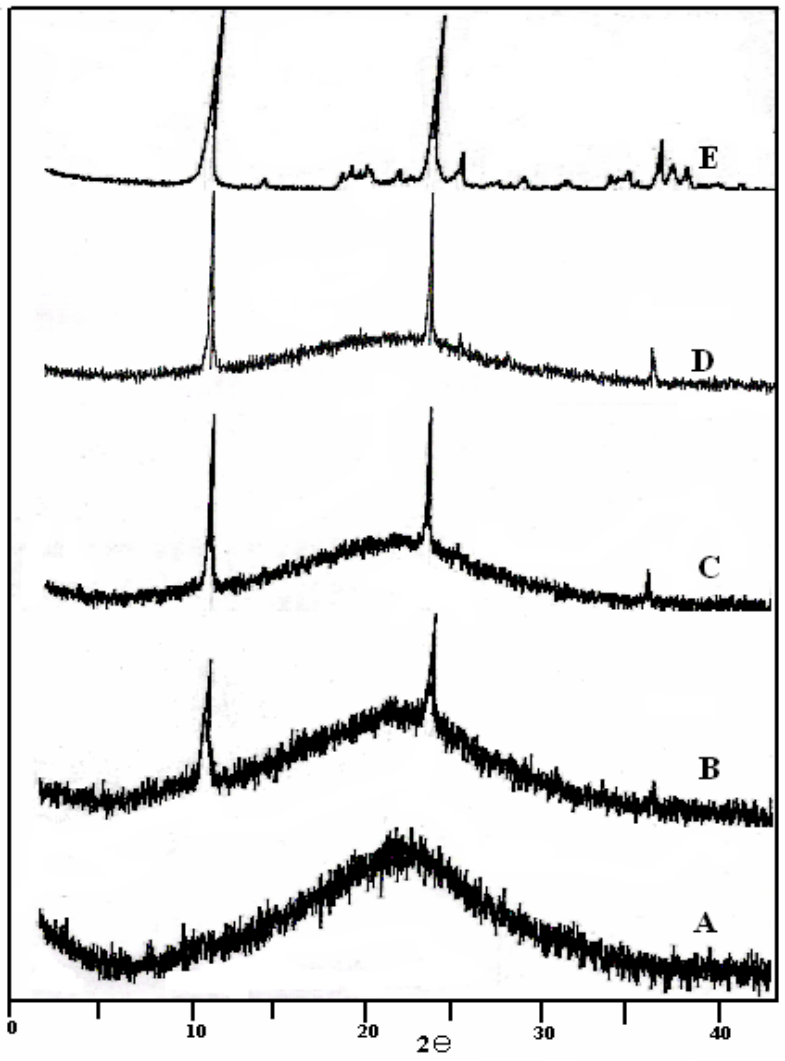

Fig. 4: X-ray diffraction pattern of: A) TFC, B) 0.001, C) 0.005, D) 0.5 wt. % TFZNC and E) pure zeolite particles.

The SEM image confirms the morphology and microstructure of the TFC and TFZNC membranes. Fig [5] shows that the smooth surfaces of Ps support membrane became rough in case of TFC and TFZNC membranes with little aggregation of zeolite nanoparticles. It is apparent that the nano zeolite is uniformly dispersed along the membrane surface when the concentration was 0.05 wt. % **(**Lu *et al.*, 2005**)**. At higher zeolite loadings, zeolite nanoparticles are visible on the membrane surface. These improvements in surface properties lead to good water permeability. Also, the nano-zeolite in the polyamide layer creates a new flow path for water

crossing through this layer. Therefore, adding nano- zeolite into polyamide increases water sorption and permeability.

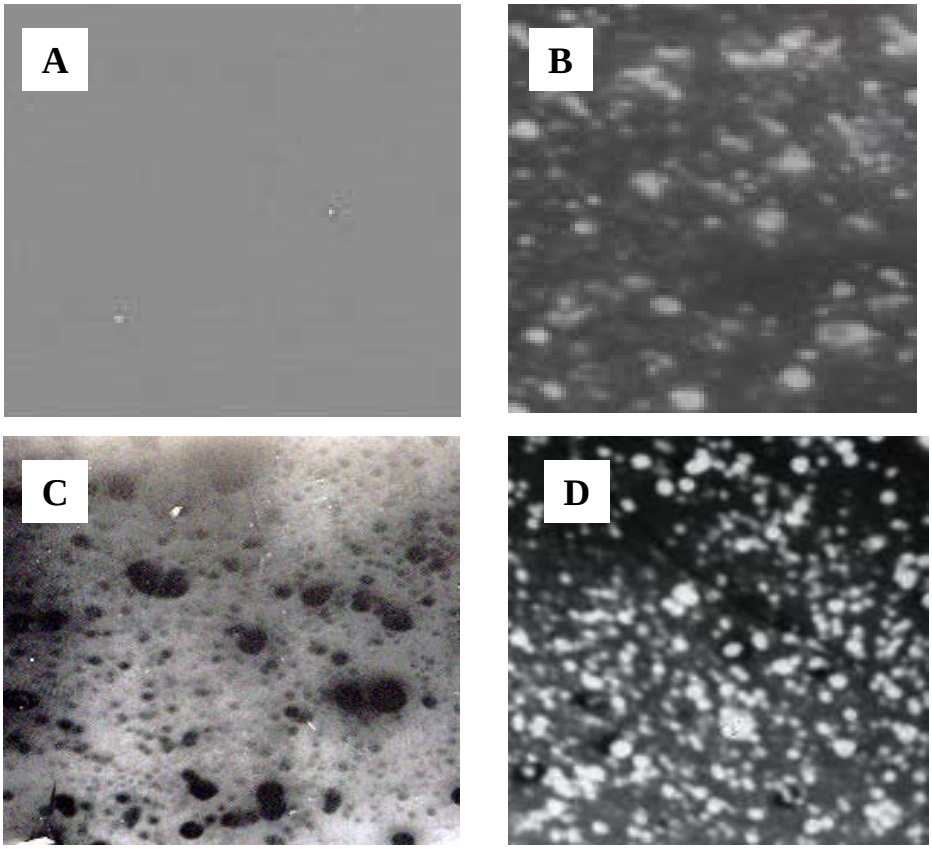

Fig. 5: SEM photographs of the surface of (A) Ps support (B) TFC (C) TFZNC (0.05 %) and (D) TFZNC (0.5 %) membranes.

3.3. Pure water permeability:

Pure water permeability (PWP) is presented for pure TFC and TFZNC (0.001 – 0.5 %) membranes, Fig [6]. All membranes exhibit high PWP which is a well-known characteristic of interfacially polymerized polyamide RO membranes as applied pressure increases. Fig [7] shows the PWP of TFC and TFZNC at different zeolite concentration (from 0.001 to 0.5 %) at applied pressure 20 bar, where PWP of the TFC membrane was 40 l/m^2.h. With increasing in zeolite loading, the PWP increases up to 63 l/m^2.h at 0.05 %. Further increasing zeolite loading had negative impacts on the TFZNC membrane permeability (49 l/m^2.h at 0.5 %). However; the high PWP of TFZNC membranes is due to small pores, super-hydrophilic, negatively charged pores (The negative charge is compensated by cations located in the intracrystalline channels and cavities) of zeolite nanoparticles which are highly attractive to water. The decreasing of PWP at high zeolite loading (0.5 %) may be due to formation a relatively thicker polyamide rejection layer.

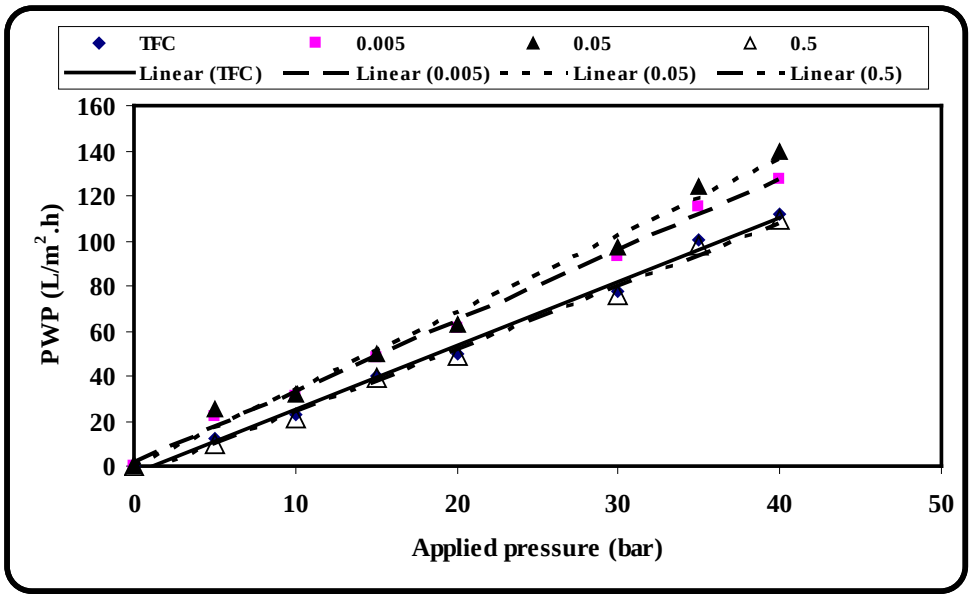

Fig. 6: Pure water permeability for different TFC membranes at different applied pressure.

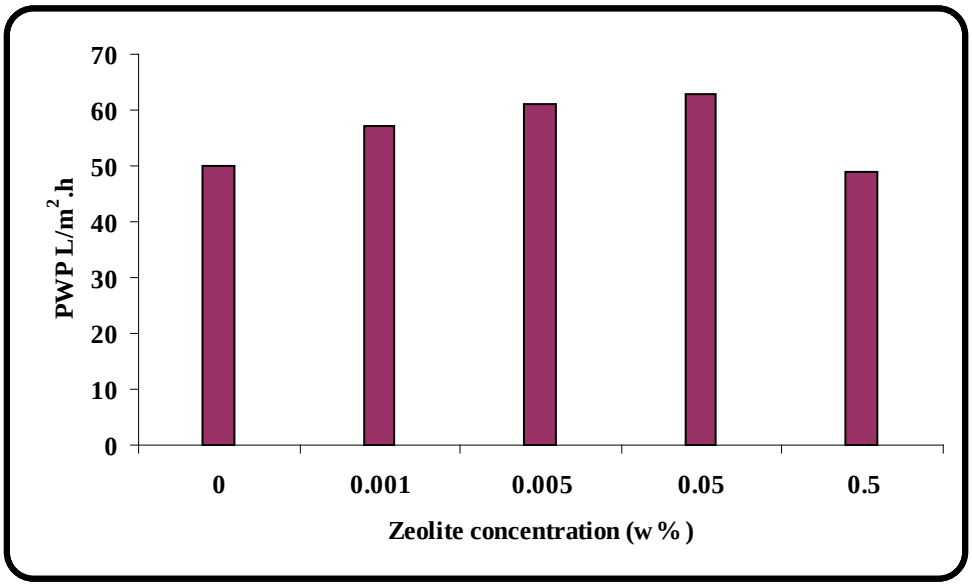

Fig. 7: Effect of zeolite loading on water permeability of the TFC membranes at applied pressure 20 bar.

3.4. Water flux and salt rejection:

Water flux and salt rejection of TFC and TFZNC membranes are compared Fig [8]. The TFZNC membrane exhibits the highest water flux with significance decreasing in salt rejection as zeolite loading increases from 0.001 to 0.05 %. The increasing of water flux of TFZNC membranes is due to the relatively smooth, hydrophilic, and negatively charged film layer **(**Vrijenhoek *et al.*, 2001**).** On the other hand, a high zeolite loading (0.5 %) may be due to formation a relatively thicker polyamide rejection layer which enhanced salt rejection. Nanoparticles like zeolite nanoparticle exhibits 0.4 nm pores which are lower than the size of the common ions presents in contaminated water and bigger than the size of a water molecule (0.278 nm). So, zeolite nanoparticles are taken to make inorganic-organic thin film nanocomposite (TFN) membranes with assumption that nanoparticles will create a straight path for flowing of pure water only retaining salt ions from salt water. Moreover, these particles are very hydrophilic, with negative charge which are highly repulsive to anions **(**Jeong *et al.*, 2007).

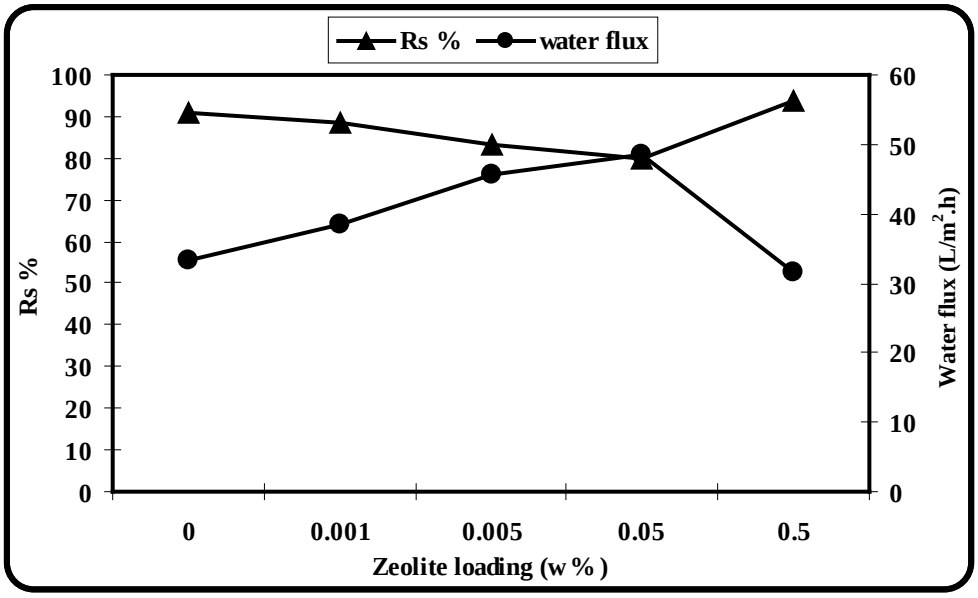

Fig. 8: Effect of zeolite loading on water flux and salt rejection of the TFC membranes.

3.5. Groundwater desalination:

Two brackish and saline groundwater samples were collected from the area between El-Quseir and Safaga, Egypt, with total dissolved solids of 2972 and 9062 mg/l at applied pressure of 20 and 30 bar, respectively, to compare the performance of TFC and TFZNC (0.05 %). Fig [9] shows the water flux and salt rejection of two membranes against samples, where R_s % slightly decreases from 87.8 to 85 % and from 93.5 to 90.5 % in presence of zeolite, whereas the water flux increases from 27.7 to 36.1 l/m^2.h and from 94.4 to 122 l/m^2.h for two groundwater samples, respectively. However, the permeate water in two cases is suitable for drinking according to WHO (TDS less than 1000 mg/l).

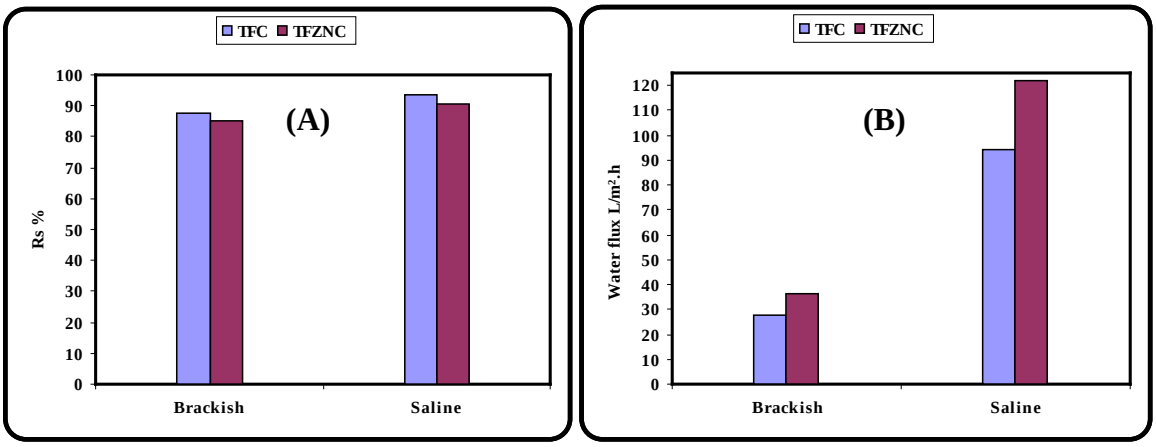

Fig. 9: Water flux and salt rejection of TFC and TFZNC membranes evaluated at 20 bar as applied pressure.

Conclusion:

This paper demonstrates formation of TFZNC membranes by interfacial polymerization technique. The formation of TFZNC was elucidated through FT-IR, XRD and SEM tools which conformed interaction between polyamide and zeolite nanoparticles. TFZNC resulted in improved permeability and water flux with slightly decreasing in salt rejection when compared to pure TFC membrane. It is found that two membranes are suitable for desalination of brackish and saline groundwater.

References

Cadotte, J.E., 1981. "Interfacially synthesized reverse osmosis membrane". US Patent, 4: 277-344.

Cadotte, J.E., R.J. Petersen, R.E. Larson, E.E. Erickson, 1980. "New thin-film composite seawater reverse-osmosis membrane". Desalination., 32: 25-31.

Dyer, A., 1988. "An introduction to zeolite molecular sieves". John Wiley & Sons, Toronto.

Ghosh, A.K., E.M.V. Hoek, 2009. "Impacts of support membrane structure and chemistry on polyamide–polysulfone interfacial composite membranes". J. Membr. Sci., 336: 140-148.

Ghosh, A.K., B.H. Jeong, X. Huang, E.M.V. Hoek, 2008. "Impacts of reaction and curing conditions on polyamide composite reverse osmosis membrane properties". J. Membr. Sci., 311: 34–45.

Gilron, J., S. Belfer, P. Vaisanen, M. Nystrom, 2001. "Effects of surface modification on antifouling and performance properties of reverse osmosis membranes". Desalination., 140: 167-179.

Hasine Kasgoz, Ali Durmus, Ahmet Kasgoz, 2008. "Enhanced swelling and adsorption properties of AAm-AMPSNa/clay hydrogel nanocomposites for heavy metal ion removal". Polym. Adv. Technol., 19: 213-220.

Huan, G., W. Wang, Q. Du, 2009. "Preparation and Characterization of a Novel Nanofiltration Membrane". Fibers and Polymers., 10(6): 797-801.

Jadav, G.L., V.K. Aswal, P.S. Singh, 2010. "SANS study to probe nanoparticle dispersion in nanocomposite membranes of aromatic polyamide and functionalized silica nanoparticles". J. Colloids Interface Sci., 351: 304-314.

Jadav, G.L., P.S. Singh, 2009. "Synthesis of novel silica–polyamide nanocomposite membrane with enhanced properties, J. Member. Sci., 328: 257-267.

Jeong, B.H., E.M.V. Hoeka, Yushan Yan, Arun Subramani, Xiaofei Huang, Gil Hurwitz, Asim K. Ghosh, Anna Jawor, 2007. "Interfacial polymerization of thin film nanocomposites: A new concept for reverse osmosis membranes". J. Membr. Sci., 294: 1-7.

Kim, I.C., J. Jegal, K.H. Lee, 2002. "Effect of aqueous and organic solutions on the performance of polyamide thin-film-composite nanofiltration membranes". J. Polym. Sci. B: Polym. Phys., 40: 2151-2342.

Kim, S.H., S.Y. Kwak, B.H. Sohn, T.H. Park, 2003. "Design of TiO_2 nanoparticle self-assembled aromatic polyamide thin-film-composite (TFC) membrane as an approach to solve biofouling problem". J. Membr. Sci., 211: 157-165.

Lee, S.H.S., J. Im, J.H. Kim, H.J. Kim, J.P. Kim, B.R. Min, 2008. "Polyamide thin-film nanofiltration membranes containing TiO_2 nanoparticles". Desalination., 219: 48-56.

Lind, M.L., A.K. Ghosh, A. Jawor, X. Huang, W. Hou, Y. Yang, E.M.V. Hoek, 2009. "Influence of zeolite crystal size on zeolite–polyamide thin film nanocomposite membranes". Langmuir., 25: 10139-10145.

Lind, M.L., B.H. Jeong, A. Subramani, X. Huang, E.M.V. Hoek, 2009. "Effect of mobile cation on zeolite–polyamide thin film nanocomposite membranes". J. Mater. Res., 24: 1624-1631.

Liu, G.K.M., B. Lin, Y. Cao, Q. Yuan, 2007. "A novel method of surface modification on thin-film composite reverse osmosis membrane by grafting poly (ethylene glycol)". Polymer., 48: 1165-1170.

Liu, L.F., S.C. Yu, Y. Zhou, C.J. Gao, 2006. "Study on a novel polyamide–urea reverse osmosis composite membrane (ICIC–MPD). I. preparation and characterization of ICIC–MPD membrane". J. Membr. Sci., 281: 88-94.

Lu Yan, Yu Shui Li, Chai Bao Xiang, 2005. "Preparation of poly (vinylidene fluoride) (pvdf) ultrafiltration membrane modified by nano-sized alumina (Al_2O_3) and its antifouling research". Polymer, 46: 7701-7706.

Clark, M.M., S. Allgeier, G. Amy, S. Chellam, F. Digiano, M. Elimelech, S. Freeman, J. Jacangelo, K. Jones, J. M. Laine, J. Lozier, B. Marinas, R. Riley, J. Taylor, M. Thompson, J. Vickers, M. Wiesner, A. Zander, 1998. "Committee report: membrane processes". J. Am. Water Work Assoc. 90; 91.

Mortier, W.J., 1982. "Structure Commission of the International Zeolite Association. Compilation of extra framework sites in zeolites". Butterworth Scientific Ltd.

Pendergast, M.T.M., J.M. Nygaard, A.K. Ghosh, E.M.V. Hoek, 2010. "Using nanocomposite materials technology to understand and control reverse osmosis membrane compaction". Desalination., 261: 255-263.

Rawajfeh, A.E.A., 2005. "Polyamide-based composite membranes. Part 1. Preparation and characterization". Desalination., 179: 265-272.

Roh, I.J., S.Y. Park, J.J. Kim, C.K. Kim, 1998. "Effects of the polyamide molecular structure on the performance of reverse osmosis membranes". J. Polym. Sci. B: Polym. Phys., 36: 1821-1830.

Sanchuan, Y., L. Meihong, L. Xuesong, G. Congjie, 2009. "Performance enhancement in interfacially synthesized thin-film composite polyamide-urethane reverse osmosis membrane for seawater desalination". J. Membr. Sci., 342: 313-320.

Singh, P.S., S.V. Joshi, J.J. Trivedi, C.V. Devmurari, A.P. Rao, P.K. Ghosh, 2006. "Probing the structural variations of thin film composite RO membranes obtained by coating polyamide over polysulfone membranes of different pore dimensions". J. Membr. Sci., 278: 19-25.

Soroko, I., A. Livingston, 2009. "Impact of TiO_2 nanoparticles on morphology and performance of crosslinked polyimide organic solvent nanofiltration (OSN) membranes". J. Membr. Sci., 343: 189-198.

United Nation, 2009. "Statistics: Graphs and Maps". [Online] Available at http://www.unwater.org/statistics.html (accessed 6 November 2009), WWW Article.

Vrijenhoek, E.M., S. Hong, M. Elimelech, 2001. "Influence of membrane surface properties on initial rate of colloidal fouling of reverse osmosis and nanofiltration membranes". J. Membr. Sci., 188: 115.

Wu, C., S. Zhang, D. Yang, X. Jian, 2009. "Preparation, characterization and application of a novel thermal stable composite nanofiltration membrane". J. Membr. Sci., 326: 429-434.

Yu, S., M. Liu, X. Liu, C. Gao, 2009. "Performance enhancements in interfacially synthesized thin-film composite polyamide–urethane reverse osmosis membrane for seawater desalination". J. Membr. Sci., 342: 313-320.

Zhou, Y., Y.U. Sa, M. Liu, C. Gao, 2005. "Preparation and characterization of polyamide–urethane thin-film composite membranes, Desalination., 180: 189-196.